

initial products. There remain many uncertainties as to the identity and rates of the secondary reactions leading to polymer formation at low temperatures and carbon formation at high temperatures.

Acknowledgment. Acknowledgment is made to the donors of the Petroleum Research Fund, administered by the American Chemical Society, for partial support of this research. This research was also supported by the Robert A. Welch Foundation and the U. S. Army Research Office. We thank H. B. Palmer and J. Troe for stimulating discussions.

References and Notes

- (1) M. H. Back, *Can. J. Chem.*, **49**, 2199 (1971).
- (2) T. Tanzawa and W. C. Gardiner, Jr., Seventeenth International Symposium on Combustion, Leeds, 1978, The Combustion Institute, 1979.
- (3) H. B. Palmer and F. L. Dormish, *J. Phys. Chem.*, **68**, 1553 (1964).
- (4) C. G. Silcocks, *Proc. R. Soc. London, Ser. A*, **242**, 411 (1957).
- (5) T. Tanzawa and W. C. Gardiner, Jr., Discussion contribution following ref 2.
- (6) G. B. Skinner and E. M. Sokoloski, *J. Phys. Chem.*, **64**, 1952 (1960).
- (7) P. Frank and Th. Just, *Combust. Flame*, in press.
- (8) Th. Just, private communication.
- (9) W. A. Payne and L. J. Stief, *J. Chem. Phys.*, **64**, 1150 (1976).
- (10) W. Lange and H. G. Wagner, *Ber. Bunsenges. Phys. Chem.*, **79**, 165 (1975).
- (11) A. L. Myerson and W. S. Watt, *J. Chem. Phys.*, **49**, 425 (1968).
- (12) M. S. B. Munson and R. C. Anderson, *Carbon*, **1**, 51 (1963).
- (13) C. F. Cullis and N. H. Franklin, *Proc. R. Soc. London, Ser. A*, **280**, 139 (1964).
- (14) W. C. Gardiner, Jr., B. F. Walker, and C. B. Wakefield in "Shock Waves in Chemistry", A. Lifshitz, Ed., Marcel Dekker, New York, 1980.
- (15) I. D. Gay, G. B. Kistiakowsky, J. V. Michael, and H. Niki, *J. Chem. Phys.*, **43**, 1720 (1965).
- (16) J. N. Bradley and G. B. Kistiakowsky, *J. Chem. Phys.*, **35**, 264 (1961).
- (17) C. F. Aten and E. F. Greene, *Combust. Flame*, **5**, 55 (1961).
- (18) G. D. Towell and J. J. Martin, *AIChE J.*, **7**, 693 (1961).
- (19) D. A. Frank-Kamenetzky, *Acta Physicochim. U.S.S.R.*, **18**, 148 (1943).
- (20) C. F. Cullis, G. J. Minkoff, and M. A. Nettleton, *Trans. Faraday Soc.*, **58**, 1117 (1962).
- (21) W. C. Gardiner, Jr., *J. Phys. Chem.*, **81**, 2367 (1977).
- (22) W. C. Gardiner, Jr., *J. Phys. Chem.*, **83**, 37 (1979).
- (23) C. S. Burton and H. Hunziker, *J. Chem. Phys.*, **57**, 339 (1972).
- (24) R. W. Wetmore and H. F. Schaefer, III, *J. Chem. Phys.*, **69**, 1648 (1978).

A FT IR Spectroscopic Study of the Ozone-Ethene Reaction Mechanism in O₂-Rich Mixtures

Fu Su, Jack G. Calvert,* and John H. Shaw

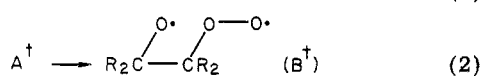
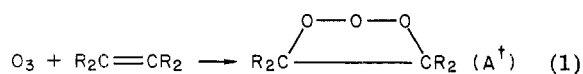
Departments of Chemistry and Physics, The Ohio State University, Columbus, Ohio 43210 (Received August 9, 1979)

Publication costs assisted by the Environmental Protection Agency

Fourier transform infrared spectroscopy has been employed to study the kinetics and products of the reaction between ozone and ethene (C₂H₄, *cis*-CDHCDH, *trans*-CDHCDH, and C₂D₄) in the ppm range in gaseous O₂-N₂ mixtures (18–26 °C, 700 torr). In addition to the expected reaction products, CO, CO₂, CH₂O, and HCO₂H, major products of the reaction were indentified as formic acid anhydride and as yet unidentified precursor to (HCO)₂O. The kinetics of formation of these products were studied in dilute mixtures of O₃ and ethene (in O₂-N₂ at 700 torr) with small amounts of CH₂O, CH₃CHO, CO, or SO₂ added. These results show that about 38% of the CH₂O₂ species formed in the O₃-ethene reaction may take part in bimolecular reactions with molecular species present in the ppm range, while about 62% fragment or rearrange in unimolecular steps. Reported here are the second-order rate constants for the O₃-ethene primary reaction and the relative rate constants for the first-order fragmentation steps of CH₂O₂ and the second-order chemical reactions of CH₂O₂ with CH₂O, C₂H₄, CO, and SO₂.

Introduction

The ozone-alkene gas-phase reactions are of special interest in atmospheric chemistry.¹ The nature of the products, the mechanism, and the rate constants for the gas-phase reactions have been studied in the extensive, pioneering efforts of Cvetanović and co-workers² and in more recent years by many other investigators from several laboratories. The earlier work was interpreted in terms of the Criegee mechanism³ in which the original molozonide fragmented to form a carbonyl compound and a reactive species which has become known as the Criegee intermediate.

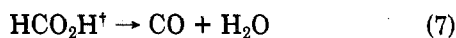
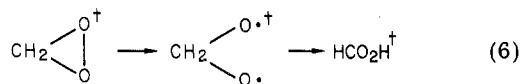
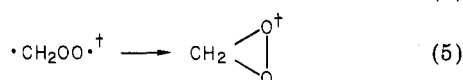
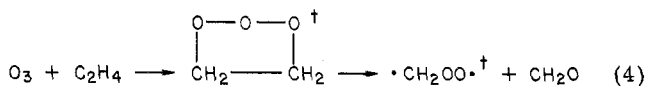


O'Neal and Blumstein⁴ suggested that the diradical intermediate product B[†] of (2) could rearrange by internal H-atom transfer together with some subsequent fragmentation steps to produce the excited molecular products and free-radicals observed experimentally.⁵ It was proposed from thermodynamic considerations and unimolecular reaction rate theory that the significant formation of the Criegee intermediate may be unimportant except for the very simplest alkene, C₂H₄, where fragmentation of the very energy-rich ozonide in (2) and (3) is most likely to occur before collisional equilibration of the initial products. However, Niki et al.⁶ showed clearly that a large fraction of the gas-phase ozonolysis of *cis*-2-butene reaction occurs via the Criegee mechanism as well.

The identification of the intermediate dioxirane (CH₂(O)₂) by Lovas and Suenram^{7a} and Martinez et al.^{7b} in the low temperature reaction of ozone with ethene provided convincing evidence for the occurrence of the Criegee mechanism for at least a major fraction of this reaction. Presumably the dioxirane formed from the initial Criegee

intermediate ($\cdot\text{CH}_2\text{OO}\cdot$) by ring closure.

Most of the researchers in recent years appear to conclude that dioxirane formed in the ozone reaction with ethylene will rearrange to a vibrationally rich formic acid molecule for which fragmentation routes (6)–(9) are ex-



pected to dominate.⁷⁻¹⁰ It is inferred that these decomposition reactions of the vibrationally rich CH_2O_2 species are so fast that bimolecular reactions of the CH_2O_2 are unimportant in the case of the gas-phase ozone-ethene reaction.

In the present work a Fourier transform infrared spectrometer has been used to follow the $\text{O}_3\text{-C}_2\text{H}_4$ reaction and to characterize the nature of the many products formed in O_2 -rich mixtures of reactants at low concentrations common to the polluted troposphere. We report here the finding that bimolecular reactions of the CH_2O_2 species formed in dilute mixtures of C_2H_4 , O_3 , and O_2 can be important with CH_2O -, CH_3CHO -, CO -, and SO_2 -containing mixtures. Some of the products formed are unusual and could be of importance in real atmospheres.

Experimental Section

The details of the experimental FT IR spectroscopic system and the large photochemical reactor have been presented elsewhere.¹¹ The path of the IR analyzing beam was set for 170 m, and the effective resolution of the spectra was 1 cm^{-1} . Product analyses and kinetic data were obtained from the infrared spectra of the reactants and products of mixtures of $\text{O}_3\text{-C}_2\text{H}_4$, $\text{O}_3\text{-C}_2\text{D}_4$, $\text{O}_3\text{-trans-CDHCDH}$, $\text{O}_3\text{-cis-CDHCDH}$, $\text{O}_3\text{-C}_2\text{H}_4\text{-CH}_2\text{O}$, $\text{O}_3\text{-C}_2\text{H}_4\text{-CH}_3\text{CHO}$, $\text{O}_3\text{-C}_2\text{H}_4\text{-CO}$, and $\text{O}_3\text{-C}_2\text{H}_4\text{-SO}_2$, in the ppm range in mixtures with added O_2 and N_2 to a total pressure of 700 torr and at temperatures from 18.6 to 25.8 °C.

The D-labeled ethylenes, formaldehyde (HDCO , D_2CO as paraformaldehyde), and formic acid (DCO_2H , HCO_2D , and DCO_2D) were products of Merck Sharp and Dohme Canada, Limited. CH_2O (as paraformaldehyde) was from Eastman and C_2H_4 from the Matheson Gas Co. (research grade, 99.98%). Formaldehyde monomer was generated from the paraformaldehyde by heating, passing the monomer vapors through a dry-ice trap, and condensing the formaldehyde monomer at liquid N_2 temperature. N_2 and O_2 were purchased from the Liquid Carbonic Co. Ozone was generated by the electric discharge of O_2 with Tesla coils.

The IR spectra of all of the labeled compounds employed in this work are shown in Figures 1–3. Lines from impurity CO_2 appears in some of the spectra (near $2300\text{--}2400 \text{ cm}^{-1}$) due to variable CO_2 background absorption in the optical path of our detection system. Also some sharp lines from D_2O impurity (between 1200 and 1600 cm^{-1}) are observable in the HCO_2D and DCO_2D spectra.

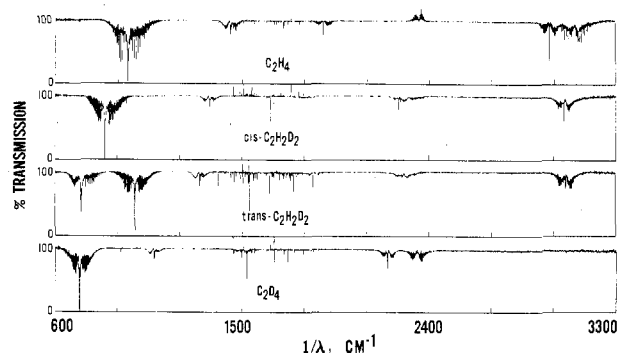


Figure 1. Infrared spectra of C_2H_4 , *cis*-CDHCDH, *trans*-CDHCDH, and C_2D_4 used in this study.

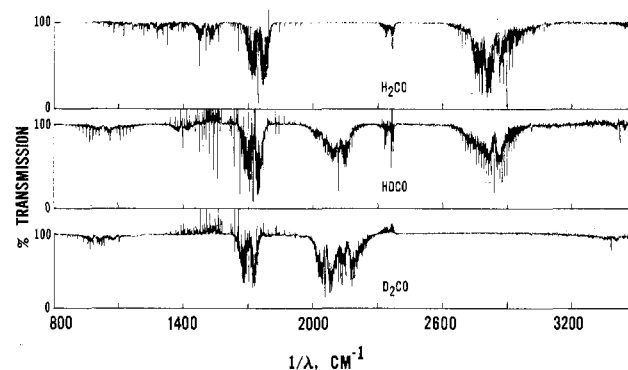


Figure 2. Infrared spectra of H_2CO , HDCO , and D_2CO used in this study.

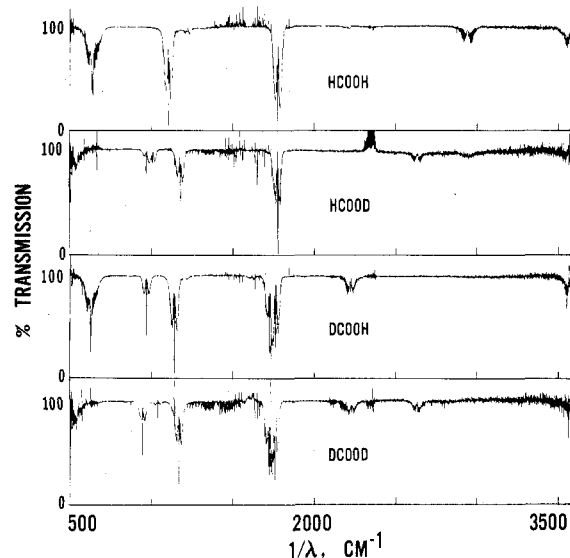


Figure 3. Infrared spectra of HCO_2H , HCO_2D , DCO_2H , and DCO_2D used in this study.

The experimental values of the extinction coefficients (base e, $\text{ppm}^{-1} \text{ m}^{-1}$ at 25 °C) for selected wavelengths employed in this work are as follows: O_3 , 9.74×10^{-4} (1055 cm^{-1}); CH_2O , 1.04×10^{-3} (2766 cm^{-1}); HCO_2H , 6.33×10^{-3} (1105 cm^{-1}); CO , 1.13×10^{-3} (average of 2176 and 2179 cm^{-1}); CO_2 , 1.40×10^{-3} (2250 cm^{-1}); SO_2 , 1.43×10^{-3} (1350 cm^{-1}); C_2H_4 , 2.05×10^{-4} (922 cm^{-1}); *cis*-CDHCDH, 4.01×10^{-4} (809 cm^{-1}); *trans*-CDHCDH, 5.99×10^{-4} (727 cm^{-1}), and C_2D_4 , 3.02×10^{-4} (701 cm^{-1}).

Results

Several different ozone-ethane experiments were carried out in this work. In the first, kinetic data from the reaction of O_3 with the various D-labeled ethenes were determined with varied pressures of O_2 and N_2 ($P_t = 700 \text{ torr}$). The

TABLE I: Summary of Stoichiometry and Rate Constant Data for the Bimolecular, Gas Phase Reactions of Ozone with the Various D-Labeled Ethenes^a

ethene used	[O ₃] ₀ , ppm	[ethene] ₀ , ppm	P _{O₂} , torr	temp, °C	Δ(O ₃)/Δ(ethene) ^b	rate constant × 10 ¹⁸ , cm ³ molecule ⁻¹ s ⁻¹
C ₂ H ₄	11.3	8.78	25.1	18.6 ± 0.2	1.00 ± 0.07	1.54 ± 0.11
C ₂ H ₄	15.2	7.37	9.1	24.0 ± 0.3	1.00 ± 0.06	1.80 ± 0.11
C ₂ H ₄	18.7	8.39	203	26.2 ± 0.6	1.01 ± 0.02	2.10 ± 0.05
C ₂ H ₄ ^c	12.5	8.97	23.6	19.7 ± 0.2	1.21 ± 0.30	1.36 ± 0.34
C ₂ H ₄ ^d	19.9	8.92	103	20.2 ± 0.2	0.97 ± 0.04	1.72 ± 0.05
C ₂ H ₄ ^e	10.4	9.22	21	25.5 ± 0.5	1.10 ± 0.28	1.68 ± 0.85
C ₂ H ₄ ^f	13.9	8.15	11	23.6 ± 0.2	1.05 ± 0.04	1.64 ± 0.07
<i>cis</i> -CDHCDH	9.32	8.84	10	25.8 ± 0.3	0.98 ± 0.02	2.15 ± 0.44
<i>trans</i> -CDHCDH	14.2	9.62	10	22.2 ± 0.5	1.01 ± 0.04	1.86 ± 0.18
<i>t</i> -CDHCDH	12.8	8.08	102	26.0 ± 0.5	1.04 ± 0.06	2.15 ± 0.14
C ₂ D ₄	19.3	7.75	10	21.4 ± 0.5	0.94 ± 0.04	1.98 ± 0.07
C ₂ D ₄	18.3	11.08	150	23.5 ± 0.5	1.02 ± 0.08	2.05 ± 0.16

^a Nitrogen gas was added to a total pressure of 700 torr; error limits shown on product ratios and rate constants are ±2σ.

^b Average ratio from the 10-20 different concentration-time points determined during the reaction. ^c CO (10.6 torr) added initially in this experiment. ^d SO₂ (4.59 ppm) added initially in this experiment. ^e CH₂O (10.2 ppm) added initially in this experiment. ^f Cl₂ (30 ppm) added initially in this experiment.

TABLE II: Product Yields in the Ozone-Ethene Reaction with Various Added Gases^a

initial reactants	P _{O₃} , torr	change in concn, ppm								ΣC _{prod} /ΣC _{react}
		-Δ(O ₃)	-Δ(C ₂ H ₄)	Δ(CH ₂ O)	Δ(CO)	Δ(CO ₂)	Δ(HCO ₂ H)	Δ((HCO) ₂ O) ^b	Δ(X) ^c	
O ₃ , C ₂ H ₄	8	7.8	8.0	4.8	2.6	(1.4)	0.33	2.3	0.50	0.92
O ₃ , C ₂ H ₄	25	5.6	5.5	4.4	2.1	1.2	0.28	1.5	0.40	1.07
O ₃ , C ₂ H ₄	200	7.7	7.7	4.3	3.0	1.6	0.32	1.4	1.1	0.92
O ₃ , C ₂ H ₄	400	8.1	8.1	4.5	3.0	1.5	0.35	1.9	0.90	0.93
O ₃ , C ₂ H ₄ , CH ₂ O ^d	21	7.2	6.3	3.6	2.9	1.6	0.53	2.2	0.08	1.05
O ₃ , C ₂ H ₄ , CO ^e	23	6.3	5.4	5.2			0.26	1.8	0.15	
O ₃ , C ₂ H ₄ , SO ₂ ^f	103	8.2	8.0	5.6	3.1	1.6	1.15	<0.03	<0.08	2.11
O ₃ , C ₂ H ₄ , SO ₂ ^g	101	7.9	6.9	5.6	2.6	1.5	0.96	<0.03	<0.08	2.43
O ₃ , C ₂ H ₄ , SO ₂ ^h	100	5.1	5.2	5.5	1.7	1.1	0.28	<0.03	<0.08	2.50

^a Initial [O₃] and [C₂H₄], about 10 ppm; total pressure (with added N₂), 700 torr; temperature, 23 ± 2 °C; final concentration measurements were made after about 50-80% reaction. ^b Calculated from the estimated extinction coefficient, ε = 3.7 × 10⁻³ ppm⁻¹ m⁻¹ (1103 cm⁻¹), base e. ^c Calculated from the estimated extinction coefficient, ε = 9.3 × 10⁻⁴ ppm⁻¹ m⁻¹ (1115 cm⁻¹), two carbon atoms per molecule X was assumed here. ^d [CH₂O]₀ = 9.68 ppm. ^e [CO]₀ = 10.6 torr. ^f [SO₂]₀ = 4.59 ppm. ^g [SO₂]₀ = 8.64 ppm. ^h [SO₂]₀ = 100 ppm.

second-order plots of some of these data for experiments near 25 °C are given in Figure 4, and the reactant loss ratios and the bimolecular rate constants for all these experiments are summarized in Table I. Given in Table II are data determined in a second series of O₃-ethene mixtures; product yields and reactant losses were derived after about 80% completion of the reaction in O₃-C₂H₄-O₂-N₂ mixtures with and without initially added CH₂O, CO, and SO₂. In an additional experiment CH₃CHO was added to O₃-C₂H₄-O₂-N₂ mixtures; the product spectra from this system are given in Figure 10.

Discussion

Reactant Stoichiometry and Bimolecular Rate Constants for the Ozone-Ethene Reaction. Our major goal in the study of the ozone-ethene system was to determine the nature of the reaction paths and ultimate fate of the CH₂O₂ fragment formed in the reaction for conditions which simulate those of the polluted troposphere. In order to test the reliability of our methods and to establish a comparison with previous work in the field, it was important for us to redetermine the kinetics of the O₃-ethene reactant disappearance in our system. A number of purely kinetic studies were carried out in this light. The characteristic infrared bands of ozone and the ethenes (C₂H₄, *cis*-CDHCDH, *trans*-CDHCDH, and C₂D₄) could be followed readily in this work by using Fourier transform infrared spectroscopy; see Figure 1. This technique provided an in situ analysis of the reacting O₃-ethene system as a function of time. The ratio of the decrease in the

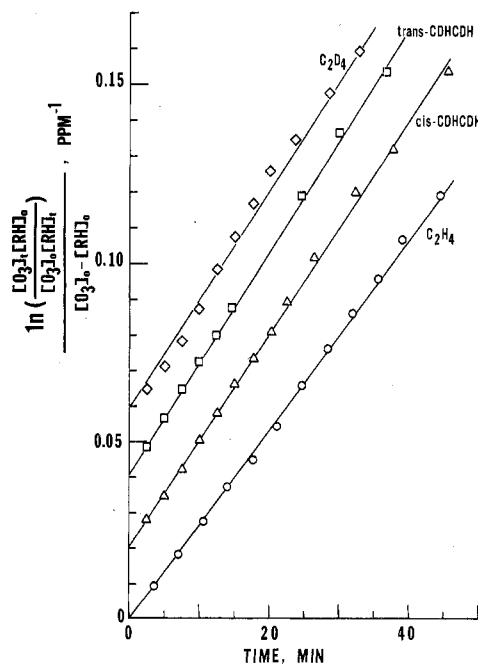


Figure 4. Plot of the second-order rate constant function vs. time which was derived from concentration-time data for the reaction of ozone with the various D-labeled ethenes; initial reactant concentrations: [O₃], 14 ± 5 ppm; [ethene], 8.5 ± 1.5 ppm; P_{N₂} + P_{O₂} = 700 torr; temperature, 25 ± 1 °C; for clarity the ordinate has been displaced upward by 0.02, 0.04, and 0.06 units for the *cis*-CDHCDH, *trans*-CDHCDH, and C₂D₄ data, respectively.

ozone concentration to that for ethene was determined at 10–20 regular intervals during the reaction of each O_3 –ethene system. The average values of the ratios $[\Delta(O_3)/\Delta(\text{ethene})]$ as determined for each of the 12 different experiments are summarized in Table I. Note that within the experimental error of measurements all of the ratios are equal to unity; error limits given here are $\pm 2\sigma$. The average of the estimates from the many experiments was $\Delta(O_3)/\Delta(\text{ethene}) = 1.03$. Note as well from the results in Table I that this one-to-one stoichiometry between reactants is maintained even in experiments at altered initial pressures of O_2 (10–200 torr) and initially added small quantities of CH_2O (10 ppm) and SO_2 (5–100 ppm). The larger ratio seen in the experiment with large amounts of added CO (10.6 torr) may be real, although the variation of the ratio with time led to the large range of values which the limits show here. We will consider this point in our later discussion.

The O_3 –ethene reactions followed second-order kinetics well as can be seen in the plots of Figure 4; these are data from similar experiments with the various ethenes in N_2 – O_2 mixtures at 700 torr pressure and $25 \pm 1^\circ C$. The slopes of these plots and other similar data for the other conditions were used to derive the second-order rate constants summarized in Table I. The near equality of the slopes for the data of Figure 4 shows that the rate constants for the O_3 –ethene reactions near $25^\circ C$ are very nearly the same for all of the D-substituted isomers: C_2H_4 , $(1.8 \pm 0.1) \times 10^{-18}$; *cis*- $CDHCDH$, $(2.2 \pm 0.4) \times 10^{-18}$; *trans*- $CDHCDH$, $(2.2 \pm 0.1) \times 10^{-18}$; C_2D_4 , $(2.1 \pm 0.2) \times 10^{-18} \text{ cm}^3 \text{ molecule}^{-1} \text{ s}^{-1}$. The only other measurement of the rate constant of D-labeled ethene of which we are aware is that of Japar et al.^{19a} who reported $k = (2.3 \pm 0.1) \times 10^{-18} \text{ cm}^3 \text{ molecule}^{-1} \text{ s}^{-1}$ for the C_2D_4 – O_3 system at $26 \pm 2^\circ C$, a value with which our estimate is in good accord. The very small effect of D substitution on the rate constant is not surprising, since the nature of the reaction site at the double bond is altered very little by D-atom substitution.

Most of the variation seen in Table I between values of the rate constant for different conditions employed in the O_3 – C_2H_4 systems studied here appears to have resulted from the small differences in temperature between the experiments. This can be seen from the Arrhenius plot of the rate constants from the C_2H_4 – O_3 reactions for the variety of different reacting mixtures in Figure 5. Also shown here as lines A, B, and C are the locus of points expected for the rate constant–temperature functions for the C_2H_4 – O_3 reaction reported by Becker et al.,¹⁶ Herron and Huie,¹⁵ and DeMore,¹⁴ respectively. The very small temperature range to which our experiments were limited does not allow an accurate estimate of the activation energy here. Our results give $E_a = 5.7 \pm 2.4 \text{ kcal mol}^{-1}$, not inconsistent with estimates from studies over much larger temperature ranges: 4.2,¹³ 4.7,¹⁴ 5.1,¹⁵ and 5.0¹⁶ kcal mol^{-1} . Determinations of the absolute value of the constants near room temperature from the previous workers^{14–17} vary by a factor of 2 as can be seen from the shifted position of the lines A, B, and C in Figure 5. The rate function of DeMore in Figure 5 represents an extrapolation of his data from much lower temperatures (-45 to $-95^\circ C$), and a small error in the activation energy could account for the difference seen here. The function of Becker et al. was derived in experiments near room temperature but at much lower pressures than we employed here (0.006–0.8 torr). Conceivably, chain processes may have enhanced the observed rate of the reaction for these conditions. The magnitude of the estimates of Herron and Huie¹⁵ (line B),

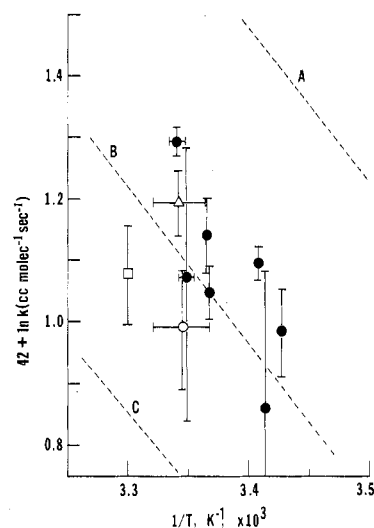


Figure 5. Arrhenius plot of the C_2H_4 – O_3 second-order rate constants; lines A, B, and C represent the locus of points defined by the rate constant functions for this reaction reported by Becker et al.,¹⁶ Herron and Huie¹⁵ and DeMore,¹⁴ respectively; points shown as closed circles are from this work; triangle, Japar et al.,^{19a} open circle, Stedman et al.;¹⁸ square, Toby et al.²⁰

Stedman et al.¹⁸ (open circle), Japar et al.^{19a} (triangle), and Toby et al.²⁰ (square) match our data reasonably well. The insensitivity of the rate constants to the added gases suggests that the secondary reactions involving free radicals, particularly noticeable in experiments at higher reactant concentrations, low O_2 pressures, and low added gas pressures^{19b,20} are unimportant here. The observed rate constants probably reflect those of the primary reaction for these conditions. Certainly the degree of consistency of our kinetic data with other recent data derived by very different methods suggests that our system is well suited to probe the details of the reaction mechanism.

The Nature of the Secondary Reactions in the O_3 – C_2H_4 – O_2 System in Simulated Polluted Atmospheres. The relatively low concentrations of the reactants used here (ppm level) and the relatively high pressures of O_2 and N_2 ($P_t = 700$ torr) were intended to be representative of those encountered in the ozone–ethene reaction within the polluted troposphere. The FT IR spectroscopic system employed here provided a unique tool for the identification of the many complex products formed in this system, and the in situ analysis has given some new and relatively unexpected results which we report here.

In Figure 6 are shown the infrared absorbance vs. $1/\lambda$ plots of a typical reacting mixture of O_3 (11.8 ppm) and C_2H_4 (9.56 ppm) in O_2 (25 torr) and N_2 (675 torr). Spectra A and B were taken after the reaction had proceeded for 2.57 and 60.25 min, respectively. The lower spectrum is the difference spectrum (B – A). Characteristic absorptions due to the expected products CO, CO_2 , CH_2O , and HCO_2H can be seen. However, there are no detectable amounts of CH_3OH , CH_3CHO , CH_2O_2 (dioxirane), HOC – H_2CHO , and the secondary ozonide of ethene (CH_2OC – H_2OO), all of which have been observed for other reaction conditions by using gas chromatography, infrared matrix experiments, microwave spectroscopy, or mass spectrometry.^{9,12}

The most surprising feature of the difference spectrum in Figure 6 is the dominance of the bands around 1812, 1760, and 1090 cm^{-1} . These correspond exactly to the main spectral features of formic acid anhydride, $(HCO)_2O$. This unusual compound was observed and first identified by Kühne, et al.,¹² for their conditions it was a very minor

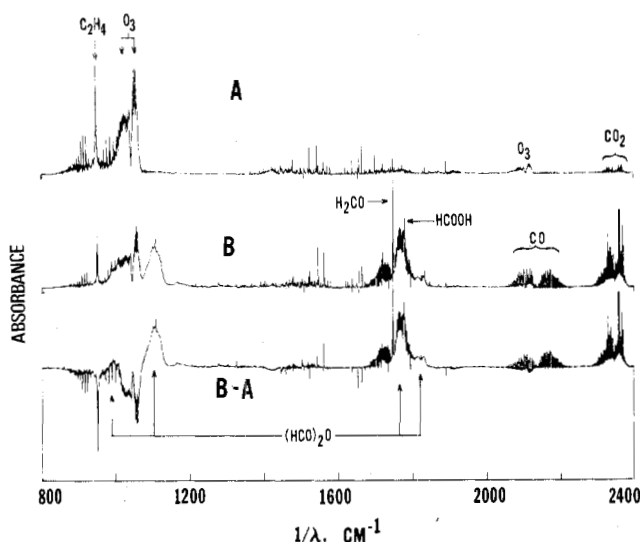


Figure 6. Absorbance vs. $1/\lambda$ plots for a gaseous mixture of initial composition: O_3 , 11.8 ppm; C_2H_4 , 9.56 ppm; O_2 , 25 torr; N_2 , 675 torr; spectrum A was taken 2.57 min after mixing; spectrum B at 60.25 min after mixing; the lower spectrum is a difference spectrum (B - A) which was used in estimation of product yields.

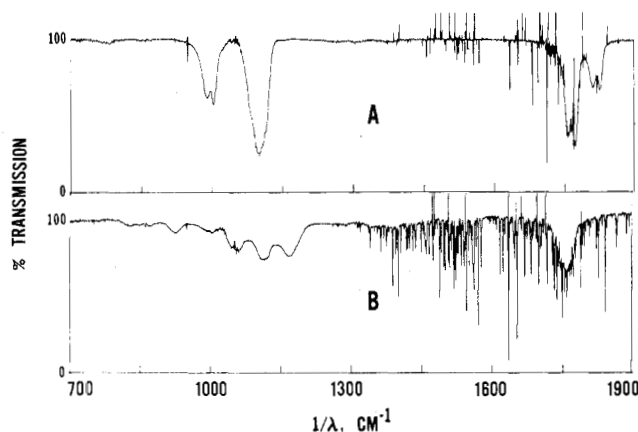


Figure 7. Infrared spectra of two newly observed major products of the $O_3-C_2H_4$ reaction; formic acid anhydride, $(HCO)_2O$, spectrum A; unknown compound X, tentatively identified as $HOCH_2OCHO$, spectrum B.

product (<0.2%) of the $O_3-C_2H_4$ reaction. They used relatively high concentrations of O_3 and C_2H_4 (5–20 torr) and observed the products condensed in an Ar matrix by infrared analysis at low temperatures. We find that the $(HCO)_2O$ is a stable, major product for our conditions. Its transmittance spectrum as derived by computer subtraction of the contributions from all other products is shown in Figure 7.

The residual spectrum B in Figure 7 is that of an as yet unidentified species (X) which is much less stable than $(HCO)_2O$ for our conditions. The absorbances due to the unknown X (1115 cm^{-1}) and those due to the $(HCO)_2O$ species (1103 cm^{-1}) vs. time are shown in Figure 8 for three different experiments. In Figure 8A the pure reactants (O_3 , $\sim 12\text{ ppm}$; C_2H_4 , $\sim 10\text{ ppm}$) were present initially. In the experiments shown in parts B and C of Figure 8, 9.68 ppm of CH_2O and 10.6 torr of CO, respectively, were added initially to the $O_3-C_2H_4$ mixtures of about the same initial concentrations employed in Figure 8A. Note that the concentration of the unknown X builds to a maximum in parts A and B of Figure 8 which occurs about 20 min into the reaction; it then decreases. With CO added the formation of X is suppressed, and its concentration appears to reach a limiting value about 30% of the maximum in parts A and B of Figure 8. There is an induction period

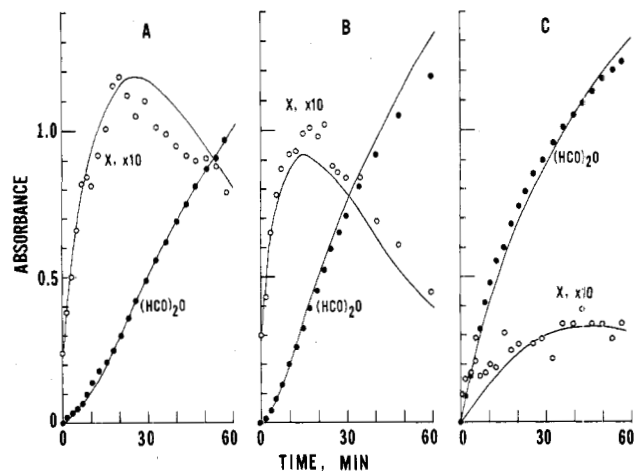


Figure 8. Time dependence of the absorbance of $(HCO)_2O$ at 1103 cm^{-1} and that for the unknown product X at 1115 cm^{-1} as determined in dilute $O_3-C_2H_4$ mixtures in O_2 and N_2 ; initial conditions were as follows: (A) O_3 , 11.3 ppm; C_2H_4 , 8.78 ppm; P_{O_2} , 25.1 torr; temp, 18.6°C ; (B) O_3 , 10.4; C_2H_4 , 9.22; CH_2O , 10.2 ppm; P_{O_2} , 21.1 torr; temp, 25.5°C ; (C) O_3 , 12.5; C_2H_4 , 8.97; P_{CO} , 10.6 torr; P_{O_2} , 23.6 torr; temp, 19.7°C ; total pressure (with added N_2), 700 torr; the solid lines in the figures are computer generated curves using the rate constants derived here.

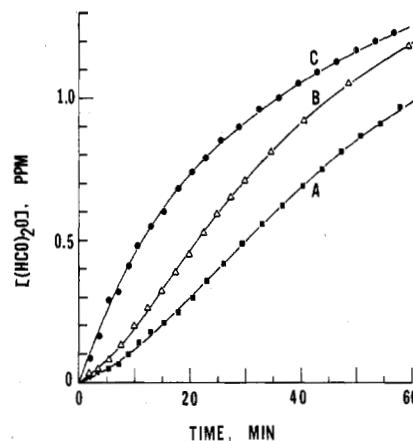


Figure 9. Comparison of the $(HCO)_2O$ product concentration vs. time plots for $O_3-C_2H_4-O_2-N_2$ mixtures; curve A, pure reactants; curve B, reactants with CH_2O added; curve C, reactants with CO added; initial concentrations as listed in Figure 8.

in $(HCO)_2O$ formation for the conditions used in Figure 8A; this is not eliminated by the addition of about 10 ppm of CH_2O (Figure 8B). On the other hand, the induction period is eliminated by the addition of a very large amount of CO (Figure 8C). The shapes of the $[(HCO)_2O]$ vs. time plots for these systems can be compared well in Figure 9. The formation of the unknown X shows no induction period in any of these experiments.

Some indications of the nature of X and its relation to $(HCO)_2O$ can be had from the rate data in Figure 8. If at selected times the rate of $(HCO)_2O$ absorbance change with time is divided by the absorbance of the unknown X at that time, a near constant is obtained. Thus the data of Figure 8A give 0.14 (4.34 min); 0.15 (7.90); 0.20 (13.23); 0.17 (20.62); 0.20 (28.52); 0.19 (39.24); 0.19 (46.25); 0.17 (56.75). This ratio for the data of Figure 8B shows a similar constancy: 0.24 (4.20 min); 0.27 (7.66); 0.30 (14.81); 0.31 (22.30); 0.28 (32.25); 0.29 (42.99); 0.22 (62.33). These results suggest that the X species decomposes to form the $(HCO)_2O$ for these conditions.

The experiment shown in Figure 8C, carried out with a large excess of CO added, gives a further insight into the nature of X. The suppression in the maximum in X seen in this case suggests that CO does compete somewhat

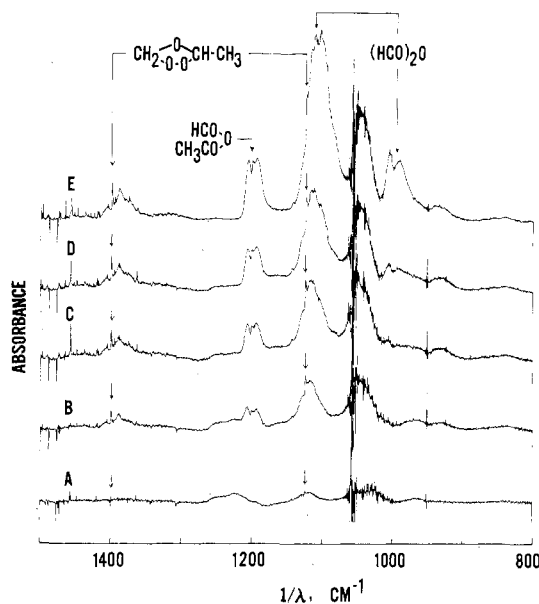


Figure 10. Product spectra of an O_3 - C_2H_4 - CH_3CHO mixture; initial concentrations: O_3 , 15 ppm; C_2H_4 , 10 ppm; CH_3CHO , 10 ppm; P_{O_2} , 100 torr; P_{N_2} , 600 torr; the IR bands of O_3 , C_2H_4 , CH_3CHO , HCO_2H , and CH_2O have been subtracted out by computer matching; times (min) after mixing: A, 1.97; B, 10.66; C, 20.38; D, 29.20; E, 116.36.

successfully for the precursor of X for these conditions. The elimination of the induction period in $(HCO)_2O$ formation for this case requires that carbon monoxide provide an additional source of this compound for these conditions.

An experiment with O_3 (15 ppm), C_2H_4 (10 ppm), and added CH_3CHO (10 ppm) gives us further helpful information. These results are shown in Figure 10. Here propylene ozonide is formed in the first few minutes of the experiment. Both formic acid anhydride and the unknown X appear only after a considerable delay. It seems clear that CH_2O_2 is the precursor of the propylene ozonide, and it follows that this same species may be a necessary reactant to form both X and $(HCO)_2O$; both of these only appear when the CH_2O product of the O_3 -ethene reaction has built up sufficiently to compete with CH_3CHO for the CH_2O_2 species.

The experiments with added SO_2 give us further clarification of the reaction mechanism. Sulfur dioxide and ozone do not react at a significant rate at low concentrations ($k \leq 8 \times 10^{-24} \text{ cm}^3 \text{ molecule}^{-1} \text{ s}^{-1}$).²¹ However, Cox and Penkett²² found that butene and the higher alkenes react with O_3 to create a species which oxidizes SO_2 rapidly to form an aerosol (H_2SO_4) product. Niki et al.²³ found that the addition of SO_2 (5 ppm) to an O_3 (5 ppm)-*cis*-2-butene (10 ppm)- CH_2O (10 ppm) mixture in air quenched the propylene ozonide formation observed in the absence of SO_2 , and the SO_2 was consumed to the extent that the ozonide formed previously. We carried out similar experiments with C_2H_4 - O_3 - O_2 - SO_2 mixtures in this work, and these results confirm the nature of the precursor to $(HCO)_2O$ and X. The time dependence of the products for one such experiment is shown in Figure 11. The $(HCO)_2O$ and unknown X are not detectable in the experiments with added SO_2 . The bimolecular rate constant based on O_3 and C_2H_4 loss here is the same as that in the absence of SO_2 within the experimental error, so SO_2 has no direct influence on the primary reaction. Furthermore, from the product yield data of Table II it can be seen that, for these experiments, $\Delta(CO) + \Delta(CO_2) + \Delta(HCO_2H) - \Delta(SO_2) \approx \Delta(C_2H_4) \approx \Delta(O_3)$. Combining this result with the observation that CO and CO_2 yields are not changed by SO_2 addition, one might conclude that the SO_2 acts to

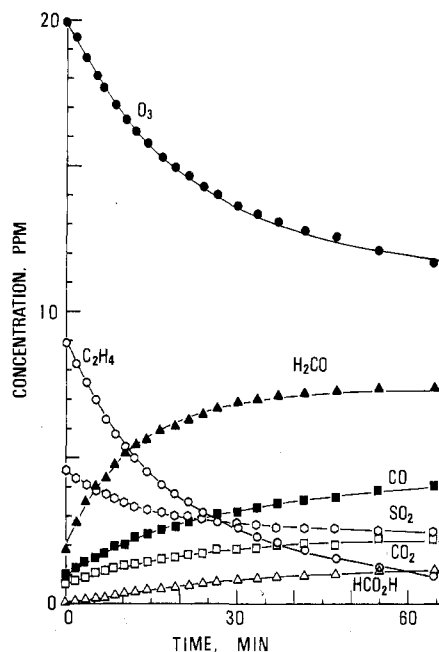


Figure 11. Product and reactant concentrations vs. time in a reacting mixture of O_3 - C_2H_4 - O_2 - N_2 with SO_2 added; initial concentrations (ppm): O_3 , 19.9; C_2H_4 , 8.92; SO_2 , 4.59; P_{O_2} , 105 torr; P_{N_2} , 597 torr.

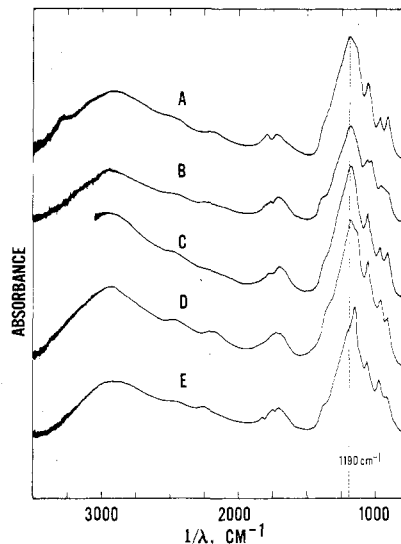
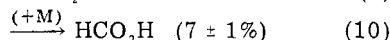
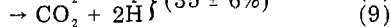
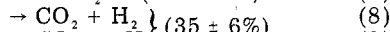
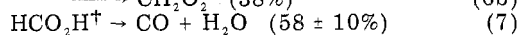
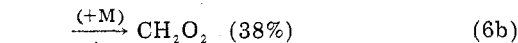
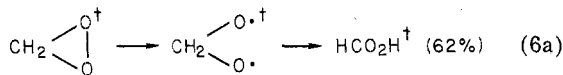
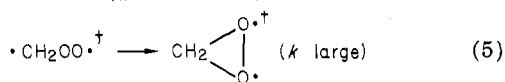
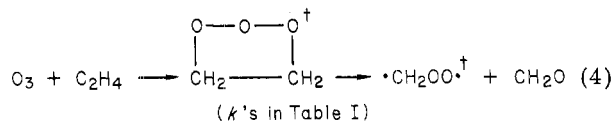


Figure 12. Infrared spectra of aerosol formed in various oxidized SO_2 mixtures: (A) photolysis of Cl_2 - H_2 - NO - SO_2 - O_2 mixture; (B) thermal reaction of O_3 , C_2H_4 , SO_2 (3.5 ppm) in O_2 - N_2 mixture; (C) thermal reaction of O_3 , C_2H_4 , SO_2 (97 ppm) in O_2 - N_2 mixture; (D) thermal reaction of O_3 , *trans*- $CDHCDH$, SO_2 in O_2 - N_2 mixture; (E) thermal reaction of O_3 , C_2D_4 , SO_2 in O_2 - N_2 mixture.

intercept some species which normally leads to $(HCO)_2O$. However, HCO_2H increases in these experiments and this simple interpretation does not provide a complete picture as we shall see.

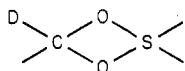
A comparison of the IR spectra of aerosols generated in Cl_2 - H_2 - NO - SO_2 - O_2 mixture photolyses, C_2H_4 - O_3 - SO_2 - O_2 , $C_2H_2D_2$ - O_3 - SO_2 - O_2 , and C_2D_4 - O_3 - SO_2 - O_2 mixtures, is given in Figure 12. The general features of these spectra are similar to one another and nearly identical with spectra observed by Niki et al.²³ who studied products from the photolysis of Cl_2 - H_2 - NO - SO_2 - O_2 mixtures. They concluded that the aerosol in their systems was H_2SO_4 with characteristic H-O bending bands at 910 and 970 cm^{-1} , O-H stretching bands at 2450 and 2900 cm^{-1} , S-O stretching bands around 1190 and 1380 cm^{-1} , S=O stretching at 1050 cm^{-1} , and a band centered at 1700 cm^{-1} assigned to the O-H bend of H_3O^+ and $(H_2SO_4H_3O)^+$ ions.

Scheme I



	relative k 's	
$\text{CH}_2\text{O}_2 + \text{C}_2\text{H}_4 \rightarrow \text{products}$	<1	(11)
$\text{CH}_2\text{O}_2 + \text{O}_3 \rightarrow \text{CH}_2\text{O} + 2\text{O}_2$	<1	(12)
$\text{CH}_2\text{O}_2 + \text{CH}_2\text{O} \rightarrow (?) \rightarrow \text{X}$	100	(13)
$\text{CH}_2\text{O}_2 + \text{SO}_2 \rightarrow \text{CH}_2\text{O}_2\text{SO}_2$ (or CH_2O + $\text{SO}_3, \text{H}_2\text{SO}_4, \text{aerosol}$)	400	(14)
$\text{CH}_2\text{O}_2 + \text{CO} \rightarrow (\text{HCO})_2\text{O}$	0.7	(15)
$\text{X} \rightarrow (\text{HCO})_2\text{O} + \text{H}_2(?)$ ($k = 0.080 \text{ min}^{-1}, 25^\circ\text{C}$)		(16)
$(\text{HCO})_2\text{O} + \text{aerosol} \rightarrow 2\text{HCO}_2\text{H} + \text{aerosol}$ (k large)		(17)

The origin of the unusual peak which we observe at 1015 cm^{-1} (weak in the spectrum of the O_3 -*trans*-CDHCDH- SO_2 - O_2 system, curve D, but stronger in the O_3 - C_2D_4 - S-O_2 - O_2 system, curve E of Figure 11) is not clear. It does not correspond to any feature of the H_2SO_4 or D_2SO_4 spectrum reported by Stopperka.²⁴ Conceivably it may relate to the D-O stretching frequency with the following linkage

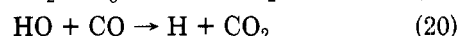
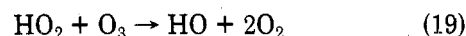
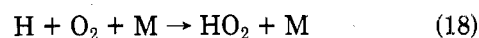


if indeed some such initial adduct is a precursor to H_2SO_4 formation in these systems.

All of these observations point strongly to the conclusion that the CH_2O_2 entity may survive decomposition and take part in secondary bimolecular reactions involving CH_2O , CH_3CHO , CO , SO_2 , and probably other species present in the polluted atmosphere. The currently accepted mechanism of the O_3 - C_2H_4 reaction should be expanded to include these seemingly important steps. The mechanism in Scheme I summarizes the kinetic information which our present results provide for the reaction of very dilute mixtures C_2H_4 and O_3 in O_2 -rich mixtures near 1 atm pressure and 25°C .

The fragmentation pattern for the $\text{CH}_2\text{O}_2^\dagger$ species observed here, which is calculated from the data on Table II, is similar to that estimated recently by Herron and Huie⁹ from relatively low pressure experiments. Their data gave the following percentages of the reaction by steps 7, 8, 9, and 10, respectively: 67, 18, 9, and 6%. Our present data do not allow an independent evaluation of the extent of the H-atom forming step 9. However, indirectly there is evidence that it does occur even at the high pressures used in our system. Note the apparent imbalance of $\Delta(\text{O}_3)/\Delta(\text{ethene})$ for the experiment at high added pressure of CO (Table I). Computer simulations employing a complete reaction mechanism including HO and HO_2 radical reactions show that the occurrence of (9) to the extent suggested by Herron and Huie can account qualitatively for the reactant imbalance seen here. A chain reaction sequence destroying O_3 can become important for the high [CO] conditions, provided that H atoms, and ultimately

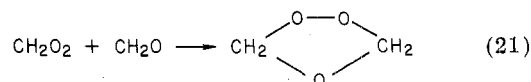
HO_2 radicals, are formed in (9):



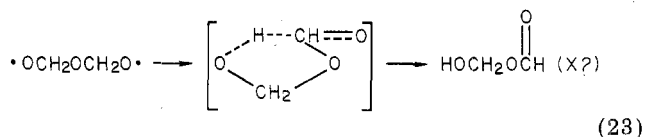
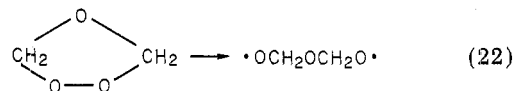
In the absence of CO the small number of HO radicals formed in (19) would react with C_2H_4 or CH_2O on a one-to-one basis, and no significant reactant imbalance would be observed with the analytical precision available to date.

According to the reaction scheme outlined here, the CH_2O_2 species formed in (4) survives decomposition and reacts with CH_2O , CH_3CHO , SO_2 , or added CO. There is always an excess of CH_2O over CH_2O_2 in our system since these species are formed in equal amounts and a large share (62%) of the CH_2O_2 species decay by reactions 7-10. Thus X would show no induction period in our usual experiment. However, $(\text{HCO})_2\text{O}$ should show a delay which reflects its formation from the initial X product. With very large CO additions, the alternate route to $(\text{HCO})_2\text{O}$, reaction 15, dominates, and the induction period is lost. The time dependences of the absorbances of X and $(\text{HCO})_2\text{O}$ as calculated by the mechanism outlined are seen as solid lines in Figure 8A-C.

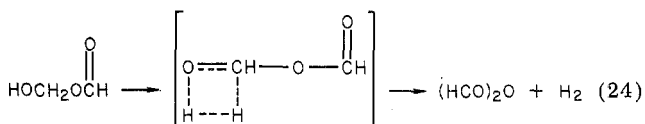
Some tentative conclusions concerning the nature of the intermediate X can be made from the data presented here. One would anticipate that the original product of a CH_2O_2 - CH_2O interaction may be the ethylene ozonide:



Although the ethylene ozonide was reported to be reasonably stable at room temperature,²⁵ it had not been observed directly in the gas phase O_3 - C_2H_4 studies by Herron and Huie⁹ and Kühne et al.¹² This indicates that the ozonide formed in reaction 21 is probably a hot molecule ($\Delta H \approx -81 \text{ kcal/mol}$) and will decompose quickly at room temperature. Note that the IR spectrum of the unknown X in Figure 7 shows a strong absorption in the region characteristic of the carbonyl stretching vibration (1700 - 1800 cm^{-1}) and several bands in the region common to C-O stretching motions (900 - 1200 cm^{-1}). A possible product can be suggested which is qualitatively consistent with these structural features. One anticipates that the ethylene ozonide formed from CH_2O_2 and CH_2O in (21) may be involved in X formation. Following the reasoning of O'Neal and Blumstein⁴ and Wadt and Goddard⁷ one would expect the ozonide to decompose as follows:

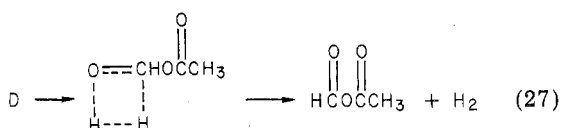
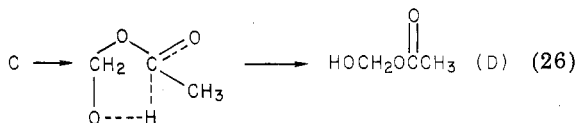
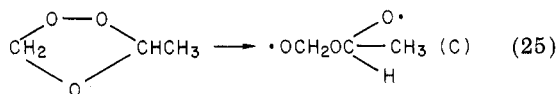


If the product of (23) is the X species observed then its thermal decomposition to $(\text{HCO})_2\text{O}$ and H_2 would presumably require passage through a four-membered ring transition state to form products which are somewhat less stable ($\Delta H_{24} \approx 22 \text{ kcal mol}^{-1}$):



The present kinetic data show that the decomposition of X has a high activation energy (about 22 kcal/mol) which is not inconsistent with this hypothesis.

The results of the $O_3-C_2H_4$ experiments with added CH_3CHO provide some additional support for this reaction scheme and the possible nature of X. The mixed anhydride of formic acid and acetic acid, $(HCO)O(OCCH_3)$, is observed in this case as well as the propylene ozonide. Presumably the former product could arise from the propylene ozonide in a similar sequence:



Regardless of the detailed structure of the unknown product X, it is highly probable that it is a molecule containing two carbon atoms. We have made this assumption in deriving the extinction coefficients for X and $(HCO)_2O$; we estimate for $(HCO)_2O$, $\epsilon = \ln(I_0/I)/cl = 3.7 \times 10^{-3} \text{ ppm}^{-1} \text{ cm}^{-1}$ at 1103 cm^{-1} , and for X, $\epsilon = 9.3 \times 10^{-4} \text{ ppm}^{-1} \text{ m}^{-1}$ (1115 cm^{-1}). Using these data, we have calculated the changes in reactant and product concentrations during a variety of $C_2H_4-O_3$ experiments. These are summarized in Table II. The carbon balance is good in all experiments but those containing SO_2 . The apparent missing carbon species in this case may result from at least two possible causes. The initial product of the $CH_2O_2-SO_2$ reaction may incorporate carbon into the aerosol (conceivably as $CH_2(O)_2SO_2$), or the SO_3 (H_2SO_4) aerosol formed may absorb CH_2O product vapors. The small differences between the spectra of the "sulfuric acid" aerosol product observed in the experiments with $C_2D_4-O_3$ and CD_3CDH-O_3 reactants (compare curves C, D, and E of Figure 12) are consistent with the initial formation of $CH_2(O)_2SO_2$ and its deuterated analogues.

The observed HCO_2H increase seen in the systems with small additions of SO_2 (Table II) appears to arise from the conversion of $(HCO)_2O$ to HCO_2H in the presence of the acid aerosol rather than the complete scavenging of the CH_2O_2 precursor by SO_2 . This view is supported by the observation that the HCO_2H yield returns to the value observed in the absence of SO_2 in the experiment with the addition of a large amount of SO_2 (100 ppm). We suggest that SO_2 at this level can entrap most of the CH_2O_2 species,

and thus the interaction of CH_2O_2 with CH_2O and its resulting formation of $(HCO)_2O$ and additional HCO_2H from reaction 17 become unimportant.

Kinetic studies of these new reactions are continuing in order to refine the rate constant estimates and further establish the details of this complex mechanism of the $O_3-C_2H_4$ reactions in air.

Acknowledgment. This work was supported by a research grant from the Environmental Protection Agency (R-806479-01-0). We are grateful to Dr. Hiromi Niki for helpful discussions related to the mechanism of the alkene-ozone reactions and a preprint of his paper before publication.

References and Notes

- (1) (a) P. A. Leighton, "Photochemistry of Air Pollution", Academic Press, New York, 1961; (b) K. L. Demerjian, J. A. Kerr, and J. G. Calvert, *Adv. Environ. Sci. Technol.*, **4**, 1 (1974).
- (2) For example, see Y. K. Wei and R. J. Cvetanović, *Can. J. Chem.*, **41**, 913 (1963).
- (3) R. Criegee, *Rec. Chem. Progr.*, **18**, 111 (1957).
- (4) H. E. O'Neal and C. Blumstein, *Int. J. Chem. Kinet.*, **5**, 397 (1973).
- (5) (a) W. A. Kummer, J. N. Pitts, Jr., and R. P. Steer, *Environ. Sci. Technol.*, **5**, 1045 (1971); (b) J. N. Pitts, Jr., B. J. Findlayson, H. Akimoto, W. A. Kummer, and R. P. Steer, *Adv. Chem. Ser.*, No. 113, 246 (1972); (c) R. Atkinson, B. J. Findlayson, and J. N. Pitts, Jr., *J. Am. Chem. Soc.*, **95**, 7592 (1973); (d) B. J. Findlayson, J. N. Pitts, Jr., and R. Atkinson, *ibid.*, **96**, 5356 (1974).
- (6) H. Niki, P. D. Maker, C. M. Savage, and L. P. Breitenbach, *Chem. Phys. Lett.*, **46**, 327 (1977).
- (7) (a) F. J. Lovas and R. D. Suenram, *Chem. Phys. Lett.*, **51**, 453 (1977); (b) R. I. Martinez, R. E. Huie, and J. T. Herron, *ibid.*, **51**, 457 (1977).
- (8) W. R. Wadt and W. A. Goddard, III, *J. Am. Chem. Soc.*, **97**, 3004 (1975).
- (9) J. T. Herron and R. E. Huie, *J. Am. Chem. Soc.*, **99**, 5430 (1977).
- (10) M. C. Dodge and R. R. Arnsts, *Int. J. Chem. Kinet.*, **11**, 399 (1979).
- (11) F. Su, J. G. Calvert, C. R. Lindley, W. M. Uselman, and J. H. Shaw, *J. Phys. Chem.*, **83**, 912 (1979).
- (12) H. Kühne, S. Vaccini, T. K. Ha, A. Bander, and Hs. H. Günthard, *Chem. Phys. Lett.*, **38**, 449 (1976).
- (13) J. J. Bufalini and A. P. Altshuler, *Can. J. Chem.*, **43**, 2243 (1965).
- (14) W. B. DeMore, *Int. J. Chem. Kinet.*, **1**, 209 (1969).
- (15) J. T. Herron and R. E. Huie, *J. Phys. Chem.*, **78**, 2085 (1974).
- (16) K. H. Becker, U. Schurath, and H. Seitz, *Int. J. Chem. Kinet.*, **6**, 725 (1974).
- (17) P. L. Hanst, E. R. Stephens, W. E. Scott, and R. C. Doerr, "Atmospheric Ozone-Olefin Reactions", Franklin Institute, Philadelphia, Pa., 1958; referenced in our ref 1a.
- (18) D. H. Stedman, C. H. Wu, and H. Niki, *J. Phys. Chem.*, **77**, 2511 (1973).
- (19) (a) S. M. Japar, C. H. Wu, and H. Niki, *J. Phys. Chem.*, **78**, 2318 (1974); (b) *ibid.*, **80**, 2057 (1976).
- (20) F. S. Toby, S. Toby, and H. E. O'Neal, *Int. J. Chem. Kinet.*, **8**, 25 (1976).
- (21) R. L. Daubendiek and J. G. Calvert, *Environ. Lett.*, **8**, 103 (1975).
- (22) (a) R. A. Cox and S. A. Penkett, *Nature (London)*, **230**, 321 (1971); (b) *ibid.*, **229**, 486 (1971); (c) R. A. Cox and S. A. Penkett, *J. Chem. Soc., Faraday Trans. 1*, **68**, 735 (1972).
- (23) H. Niki, P. D. Maker, C. M. Savage, and L. P. Breitenbach, *J. Phys. Chem.*, **84**, 14 (1980); the authors are grateful to Dr. Niki for a preprint of this work.
- (24) V. K. Stopperka, *Z. Anorg. Allg. Chem.*, **344**, 263 (1966).
- (25) L. A. Hull, I. C. Hisatsune, and J. Heicklen, Report No. 244-72 of the Center for Air Environment Studies of the Pennsylvania State University, University Park, Pa.